Cellular Signalling 23 (2011) 920–927

Contents lists available at ScienceDirect

Cellular Signalling

journal homepage: www.elsevier.com/locate/cellsig

Differential activities of the *Drosophila* JAK/STAT pathway ligands Upd, Upd2 and Upd3

Victoria M. Wright [a,b], Katja L. Vogt [b], Elizabeth Smythe [b], Martin P. Zeidler [a,b,*]

[a] MRC Centre for Developmental and Biomedical Genetics, The University of Shef!eld, Firth Court, Shef!eld, S10 2TN, UK
[b] Department of Biomedical Science, The University of Sheffield, Firth Court, Sheffield, S10 2TN, UK

ARTICLE INFO

Article history:
Received 16 November 2010
Received in revised form 5 January 2011
Accepted 17 January 2011
Available online 22 January 2011

Keywords:
STAT92E
JAK2
Unpaired
Drosophila
RNAi

ABSTRACT

JAK/STAT signalling in vertebrates is activated by multiple cytokines and growth factors. By contrast, the *Drosophila* genome encodes for only three related JAK/STAT ligands, Upd, Upd2 and Upd3. Identifying the differences between these three ligands will ultimately lead to a greater understanding of this disease-related signalling pathway and its roles in development. Here, we describe the analysis of the least well characterised of the Upd-like ligands, Upd3. We show that in tissue culture-based assays Upd3–GFP is secreted from cells and appears to interact with the extracellular matrix (ECM) in a similar manner to Upd, while still non-autonomously activating JAK/STAT signalling. Quantification of each of the Upd-like ligands in conditioned media has allowed us to determine the activity of equal amounts of each ligand on JAK/STAT *ex vivo* and reveals that Upd is the most potent ligand in this system. Finally, investigations into the effects of ectopic expression of Upd3 *in vivo* have confirmed its ability to activate pathway signalling at long-distance.

1. Introduction

The JAnus Kinase (JAK)/Signal Transducer and Activator of Transcription (STAT) cascade mediates intracellular signalling in response to multiple cytokines and growth factors. In the canonical model of JAK/STAT signalling, binding of extracellular ligand to the receptor induces a conformational change leading to the activation of receptor-associated JAK kinases. The activated JAKs trans-phosphorylate tyrosine residues on the receptor and themselves, creating docking sites for the SH2 domain containing STATs. Cytoplasmic STATs are then recruited to the membrane and activated by tyrosine phosphorylation allowing dimerisation to occur via interactions between their SH2 domains and phospho-tyrosines. The dimerised STATs then translocate to the nucleus to regulate transcription [reviewed in 1].

In vertebrates, misregulation of JAK/STAT signalling has been associated with several diseases including haematopoietic disorders [2], leukaemias [3] and cancers [4] due to its roles in cellular proliferation, haematopoiesis and the immune response. These roles of JAK/STAT signalling have also been conserved throughout evolution with alterations in JAK/STAT activity in invertebrates such as *Drosophila*, also affecting cell proliferation [5], haematopoieic cell regulation and differentiation [6,7]. In addition, the *Drosophila* JAK/STAT cascade also plays roles in embryonic development, and stem cell maintenance [reviewed in 8,9].

An advantage of studying JAK/STAT in *Drosophila* is the presence of a complete and yet low complexity version of the canonical JAK/STAT pathway, encoding a single receptor called *domeless* (*dome*) [10,11], a JAK kinase, *hopscotch* (*hop*) [12] and a STAT transcription factor, referred to as *stat92E* [13,14]. JAK/STAT signalling in vertebrates can be activated by a large range of ligands including, interferons, interleukins, cytokines and growth factors whereas the *Drosophila* genome encodes only three ligands, Unpaired/Outstretched (henceforth termed Upd) [15], Upd2 [16] and Upd3 [17]. Sequence alignments suggest that the *Drosophila* JAK/STAT ligands show some similarity to the vertebrate leptins [18], and the predicted secondary structure for Upd is similar to that of other cytokines with stretches of ∝-helices [15] suggesting a similar function.

The *upd* locus was initially suggested as a potential JAK/STAT pathway component as loss-of-function mutants produce embryonic segmentation defects similar to both *hop* and *stat92E* mutants [15]. Biochemical characterisation confirmed Upd as an activator of the JAK/STAT pathway with Hop tyrosine phosphorylation observed only in the presence of ectopic Upd expression [15]. Subsequent *in silico* searches identified two Upd-like homologues referred to as Upd2 and Upd3 [16,17] and both *ex vivo* and *in vivo* JAK/STAT assays have also shown that Upd2 is capable of activating JAK/STAT signalling [16]. Although not yet studied in detail, Upd3 has also been shown to play a role in JAK/STAT signalling. Upon septic injury, Upd3 is up-regulated and is responsible for the JAK/STAT activation that results in the expression of the stress response actor TotA [17].

Signalling in response to Upd and Upd2 occurs non-autonomously as tissue culture-based assays have demonstrated that both ligands can be secreted into media to activate JAK/STAT signalling in cells containing a JAK/STAT luciferase reporter [15,16]. In addition, long-

* Corresponding author at: Department of Biomedical Science, The University of Sheffield, Firth Court, Sheffield, S10 2TN, UK. Tel.: +44 114 222 6093; fax: +44 114 276 5413.
E-mail address: m.zeidler@sheffield.ac.uk (M.P. Zeidler).

0898-6568/$ – see front matter © 2011 Elsevier Inc. All rights reserved.
doi:10.1016/j.cellsig.2011.01.020

range pathway activation has been observed, in the *Drosophila* eye in response to ectopic Upd expression [19,20] and in the embryo with Upd2 expression in the ectoderm activating the *in vivo* JAK/STAT activity reporter, *dome-MESO*, in the mesoderm [16]. By comparison, little is known about the mechanisms by which Upd3 can activate the JAK/STAT pathway. Furthermore, determining how each of the ligands results in the downstream effects of JAK/STAT signalling will be important in understanding the pathway roles in development and how misregulation of JAK/STAT can result in disease.

Here, we investigate the mechanism by which Upd3 can activate JAK/STAT signalling. Using tissue culture-based assays we show that Upd3 is a secreted molecule that can activate the JAK/STAT pathway non-autonomously. In addition, we have generated media conditioned with specific Upd-like molecules and developed assays to quantify the amount and activity of each ligand. We show that there are differences in the strength and temporal dynamics of each of the Upd-like ligands to activate an *in vitro* JAK/STAT reporter with Upd being the most potent and Upd2 producing the longest response. Finally we move our analysis *in vivo* and show that ectopic expression of Upd3 in different *Drosophila* tissues results in similar effects to the expression of Upd, with studies in the ovary demonstrating that Upd3 can activate the JAK/STAT pathway non-autonomously *in vivo*.

2. Results

2.1. Upd3, a secreted protein that activates JAK/STAT in cell culture-based assays

It has been shown that Upd and Upd2 are secreted proteins [15,16] and both cytokines can non-autonomously activate signalling at a distance [16,20]. By comparison, relatively little is known about Upd3, the nature of its secretion and ability to activate the JAK/STAT pathway.

The *upd3* gene is situated between *upd* and *upd2* at polytene band 17A on the X chromosome and consists of 4 exons (Fig. 1A) encoding the smallest of the Upd-like ligands with a length of 401 amino acids and includes several predicted N-linked glycosylation sites (Fig. 1B). Post-translational N-linked glycosylation has been previously predicted for Upd [15]. Homologues of *Drosophila melanogaster* (*Dmel*) Upd3 are encoded by all sequenced *Drosophilid* genomes (Fig. 1C and D) with the *Dmel* Upd3 remaining more closely related to all other Upd3 homologues than to the other *Dmel* Upd-like ligands (Fig. 1D) suggesting that the Upd group of ligands radiated into three distinct molecules before the evolutionary divergence of the *Drosophilidae*. However, Upd-like proteins diverge quite considerably between these closely related flies (Fig. 1D) and no *upd*-like genes could be identified in other insects suggesting that Upd-like ligands represent a rapidly evolving group of proteins.

Given that a secreted ligand should include an N-terminal signal sequence we examined *Dmel* Upd3 for such a motif. However, SignalP 3.0 [21] predicts an N-terminal anchor sequence of 63 amino acids (C-terminal boundary indicated by the light grey arrow Fig. 1C), suggesting that Upd3 may not be secreted—a striking contrast to the signal sequence correctly predicted for *Dmel* Upd. However, analysis of other Upd3-like molecules found that *Drosophila yakuba* Upd3 contains a high confidence signal sequence located at amino acid 29 and is found at the N-terminus of a region conserved in most Upd3s (black arrow in Fig. 1C). As such, this predicted site may well represent the physiological cleavage site *in vivo*.

Given the previously described differences between the cell localisation and secretion of Upd and Upd2 [16], we first investigated whether Upd3 is in fact secreted. We therefore generated a C-terminal GFP fusion construct, *pAc–upd3–GFP* (see Experimental procedures) and transiently transfected this into *Drosophila* Kc_{167} cells. Upd3–GFP can be visualised both within the cytoplasm and also as a 'halo' around the cell (Fig. 2A), an effect previously described for Upd–GFP (Fig. 2A, [16]). Extracellular Upd3–GFP can only be visualised at the most basal confocal sections and, given the similarity to Upd–GFP which has previously been shown to be ECM-associated [15,16], may indicate an interaction between Upd3 and the extracellular matrix (ECM).

We next used transcriptional reporters of JAK/STAT activity in Kc_{167} cells to further characterise Upd3. The *6x2xDrafLuc* reporter contains twelve STAT92E binding sites upstream of the firefly luciferase gene to report STAT92E activity via changes in firefly luciferase activity [22]. Transfection of plasmids constitutively expressing Upd, Upd2 or Upd3 GFP fusion proteins significantly increased *6x2xDrafLuc* activity when compared to cells transfected with empty vector (Fig. 2B) demonstrating that Upd, Upd2 and Upd3 can all activate STAT92E in this tissue culture model.

Given the ambiguity regarding the signal sequence of *Dmel* Upd3 we next designed a paracrine assay to determine if Upd3 expression in one population of cells is capable of signalling to a second population of cells. Using Upd and Upd2 paracrine assays as a baseline, Upd3 demonstrated a similar ability to signal non-autonomously and was able to induce a 15-fold increase in STAT92E activity compared to control cells transfected with an empty vector (Fig. 2C).

Finally assays were set up in which media previously conditioned by cells expressing the Upd-like ligands is added to cells transfected with the *6x2xDrafLuc* reporter (Fig. 2D). It has previously been shown that the addition of heparin to media being conditioned with Upd can increase the amount of soluble ligand released into the media, presumably by competing with the ECM for Upd binding (Fig. 2D, [16]). By contrast, heparin has no significant effect on media conditioned by Upd2 which, when considered together with the cell localisation results, suggests that Upd2 does not interact with the ECM. However, while Upd3 appears to condition media, the addition of heparin almost completely ablates activity (Fig. 2D)—a result opposite to Upd. Given the normal signalling elicited by Upd and Upd2 in the presence of heparin, this effect is unlikely to be caused by a general effect of heparin on the Dome receptor. Rather, heparin could inhibit Upd3 production, directly affect Upd3 or interfere with the Upd3/Dome interaction. In order to differentiate between these possibilities we treated Upd3 conditioned media with heparin and added this to cells transfected with the *6x2xDrafLuc* reporter (Fig. 2E). Compared to mock, Upd3 conditioned media gives around a 17-fold increase in reporter activity while media with added heparin is essentially inactive (Fig. 2E). This suggests that the effect occurs after secretion and that heparin impairs Upd3 either directly or via its interaction with Dome. A similar sensitivity to heparin has been previously reported for human cytokines [23] and given this interaction heparin was not used in subsequent experiments.

We have demonstrated that Upd3 is a secreted cytokine that is able to activate STAT92E *ex vivo*. In order to determine if Upd3 signals through the same canonical pathway as Upd we undertook autocrine assays as above following knockdown with dsRNA targeting known JAK/STAT pathway components [22,24]. RNAi knockdown of the core pathway components *hop*, *stat92E* and *dome* resulted in a significant decrease in JAK/STAT pathway activity in response to all three ligands (Fig. 2F). In addition, knockdown of the negative regulators, *socs36E* and *ptp61F* result in a significant increase in JAK/STAT reporter activity (Fig. 2F). These results confirm that all three ligands, including Upd3, activate signalling via a single activating receptor, JAK and STAT molecule. Furthermore, known regulators such as SOCS36E and Ptp61F mediate the down-regulation of Upd3-activated pathway signalling as has previously been shown for Upd and Upd2 [22,24].

2.2. The Upd-like ligands exhibit different abilities to activate JAK/STAT signalling

Although the JAK/STAT assays (Fig. 2B–E) demonstrated an activity for each of the Upd-like ligands, they do not allow the absolute ability of each of the ligands to stimulate pathway activity to be determined. We

therefore developed an anti-GFP sandwich ELISA to quantify GFP-tagged protein in samples of conditioned media. A large batch of media sufficient for subsequent experiments was prepared and the concentrations of each ligand were measured. In this batch, levels of Upd2 (145 nM) were 33 times higher than Upd (4.4 nM) and 26 times Upd3 (5.6 nM). Based on these findings, we next prepared a range of defined

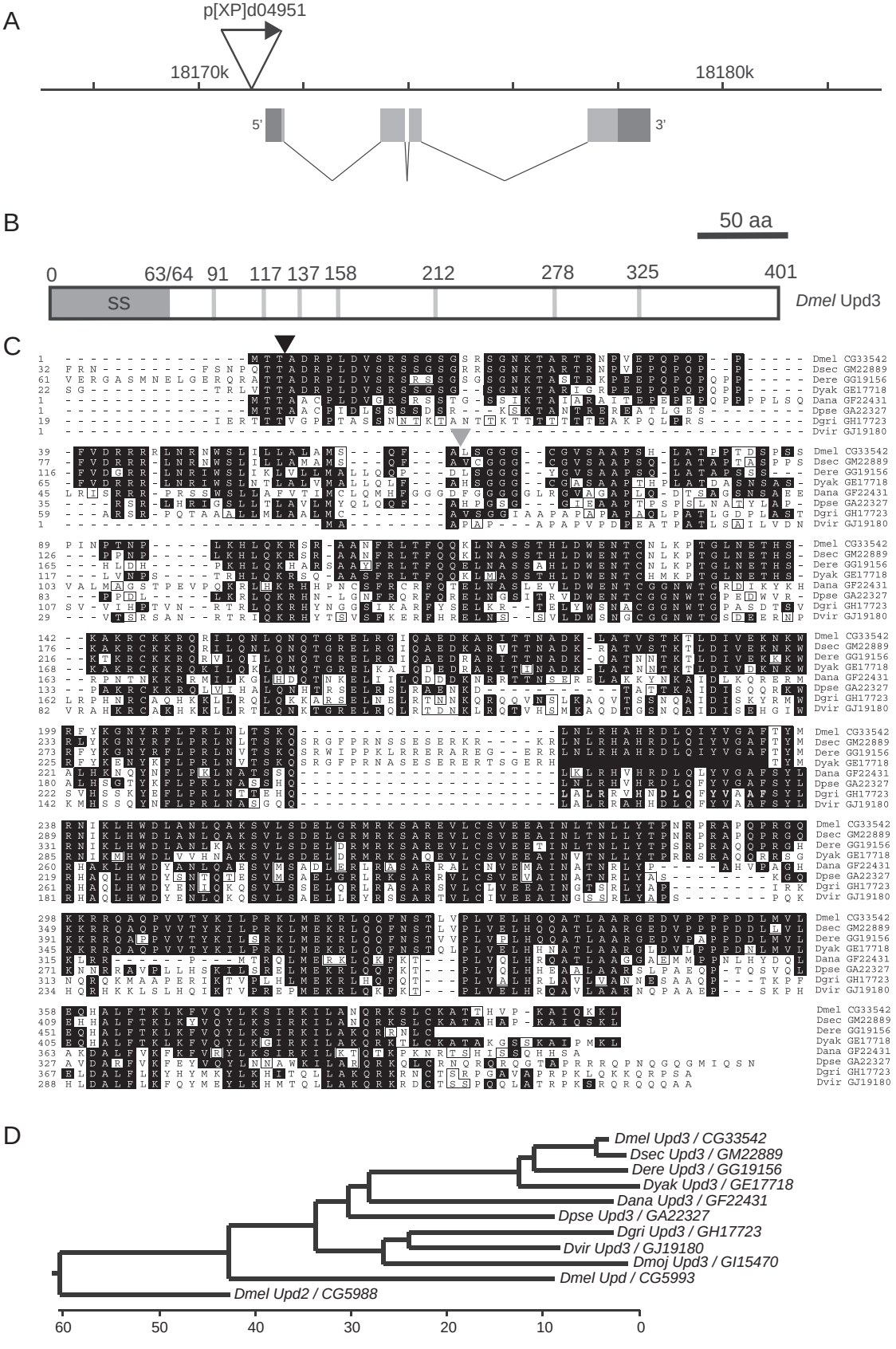

ligand concentrations (using mock conditioned media to dilute) and measured the resulting effect on *6x2xDrafLuc* reporter activity (Fig. 3A). At equivalent concentrations, Upd is significantly more potent than Upd3 while both Upd and Upd3 are able to stimulate significantly higher levels of STAT92E activity than Upd2. Indeed, even 0.5 nM of Upd is sufficient to stimulate reporter expression 15-fold above control. These results demonstrate clear differences in the activity of each of the Upd-like ligands as judged by their ability to activate JAK/STAT signalling. However, two potential caveats should be noted: firstly, the luciferase reporter represents the activity of the downstream STAT92E transcription factor and not the affinity of ligand for receptor. Secondly, while luciferase reporter activity is dependent on Upd-like ligands, quantification was based on the GFP portion of the fusion proteins rather than directly on the specific activity of the Upd ligands.

Given the co-expression of Upd-like molecules *in vivo* [16] we tested for potential synergistic (or inhibitory) effects between the Upd-like ligands. To explore this we used 1 nM of each ligand to stimulate cells containing *6x2xDrafLuc* either separately or in combination (Fig. 3B). As expected, the reporter activation elicited by 1 nM of each ligand recapitulates the results found in Fig. 3A. However, mixing of Upd-like ligands (striped bars in Fig. 3B) generated no detectable synergistic or inhibitory effects and all ligands appear to act in a purely additive manner (Fig. 3B).

To examine the temporal dynamics of signalling activation by each of the Upd-like ligands we next undertook a time-course utilising the *10xSTATluc* STAT92E activity reporter [24]—a reporter that produces a much larger signal in response to JAK/STAT signalling making it easier to detect small increases in pathway activation. Conditioned media containing 4 nM of each ligand was added to cells as a 30 min pulse before extensive washing and a chase for the times indicated (Fig. 3C). As shown previously, Upd activates signalling at higher levels than the same concentration of Upd2 or Upd3. Moreover, these results show that the temporal dynamics of signalling by Upd and Upd3 are similar with reporter activity elicited by both ligands peaking around 6–10 h and decreasing by 22 h. By comparison, activation by Upd2 is lower, but appears to be maintained and is still increasing at the 22 h time point. To confirm this result and determine when Upd2-induced stimulation reaches its maxima we carried out a further time-course, which showed that the response to Upd2 has begun to decrease by 48 h (Fig. 3D). However, even after 144 h reporter activity is still significantly above basal levels suggesting that secondary responses may increase the levels of JAK/STAT signalling in these cells after the initial exposure to Upd2.

2.3. Upd3 can signal non-autonomously upon ectopic expression in vivo

Having demonstrated that Upd3 can activate JAK/STAT signalling in cultured cells, we next set out to establish if Upd3 can activate the pathway *in vivo*. The P-element, *P[XP]d04951*, is situated 5′ to the *upd3* coding region (Fig. 1A) and contains UAS sites which should result in ectopic expression of Upd3 in the presence of Gal4. Consistent with this, quantitative RT-PCR on mRNA isolated from 0 to 16 h embryos revealed a large and specific increase in *upd3* expression driven by *Actin–Gal4* in the *P[XP]d04951* genetic background (Supplementary Fig. 1A).

Having established that *P[XP]d04951* can drive overexpression of *upd3* (henceforth referred to as *UAS–upd3*) we set out to determine if Upd3 can activate JAK/STAT signalling *in vivo*. Upd plays an important role in the development of the *Drosophila* eye and loss of Upd or other members of the JAK/STAT pathway result in a reduction in eye size [5] while *GMR–Gal4/UAS–Upd*, which drives Upd expression in the third instar larval eye imaginal disc, is sufficient to increase cellular proliferation and cause an enlarged adult eye phenotype [5,20]. We therefore used *GMR–Gal4* to drive the expression of Upd, Upd3 and GFP. As expected, Upd3 expression increases *Drosophila* eye size compared to controls expressing GFP (Fig. 4A–C) suggesting that Upd3 can activate JAK/STAT signalling in the *Drosophila* eye [5]. Although eye overgrowth is associated with ectopic JAK/STAT pathway activation, it does not represent a direct readout of pathway activity. We therefore used the *10xSTAT–GFP in vivo* reporter [25] to examine the pattern of pathway activation within the embryonic hindgut. The *10xSTAT–GFP* reporter, based on the *10xSTATluc* reporter used above, accurately mirrors JAK/STAT pathway activity *in vivo* [25] reporting pathway activation in the anterior portion of the wild type stage 13 embryonic hindgut (Fig. 4D–D″). Using *brachyenteron–Gal4* [26] to drive *UAS–Upd* and *UAS–Upd3* expression throughout the hindgut (see Supplementary Fig. 1B for expression pattern of *byn-Gal4*) we see a strong up-regulation in *10xSTAT–GFP* activity along the length of the large intestine (Fig. 4E–F″) mediated by both Upd and Upd3 demonstrating that Upd3 can stimulate STAT92E activity *in vivo*.

Finally, we set out to determine whether Upd3 is capable of signalling non-autonomously using a developmental model involving ectopic expression of Upd3 in the *Drosophila* ovary. Upd-mediated JAK/STAT activation is required to non-autonomously recruit follicle cells to the migrating border cell cluster [27,28] with ectopic overexpression of Upd in polar cells sufficient to recruit extra follicle cells to invade the nurse cells which subsequently separate from the border cell cluster during migration [28]. Here, ectopic expression of Upd, Upd3 and GFP was driven in polar cells using the *E132–Gal4* line (arrowheads in Fig. 4G)[25,29]. *E132–Gal4*-mediated expression of both Upd and Upd3 result in the recruitment of extra follicle cells when compared to expression of GFP (marked by white arrows Fig. 4H and I). Use of an alternative follicle cell driver, *slbo–Gal4* [30] produced similar phenotypes when crossed to both *UAS–Upd* and *UAS–Upd3* and allowed quantification of this phenotype (Table 1). As these excess cells are not observed upon expression of GFP, this phenotype indicates that the effect is specific to the activation of JAK/STAT signalling by ectopic ligand expression and confirms that Upd3 is capable of acting at a distance to activate JAK/STAT pathway signalling *in vivo*.

3. Discussion

We have shown that the ligand, Upd3 is a secreted molecule capable of activating JAK/STAT pathway signalling in *Drosophila*. We show that Upd3 is secreted and can act non-autonomously, is likely to interact with the ECM and is sensitive to heparin. We show that Upd3 signals through the canonical JAK/STAT pathway and that the three Upd-like ligands do not appear to act synergistically *ex vivo*. We also present the first quantification of the Upd, Upd2 and Upd3 ligands and demonstrate significant differences between the ligands in their ability to activate the strength and duration of JAK/STAT pathway signalling. Finally, we have shown that Upd3 is capable of activating JAK/STAT *in vivo* by utilising the *10xSTATGFP* reporter in the embryonic hindgut and that Upd3 can signal non-autonomously when ectopically expressed in the *Drosophila* ovary.

Fig. 1. Molecular organisation and conservation of *upd3*. (A) Schematic representation of the genomic region encoding *upd3*, where dark grey boxes represent 5′ and 3′ UTRs, with coding sequence represented by light grey boxes. The position and orientation of the *P[XP]d04951* P-element insertion is shown to be 5′ to the *upd3* coding region (not to scale). (B) The Upd3 protein, the predicted signal/anchor sequence (SS) is indicated by the grey box and predicted glycosylation sites marked by light grey lines and the amino acid number. (C) Alignment of the predicted amino acid sequences of the Upd3 proteins encoded by the sequenced *Drosophilid* genomes. Grey arrowhead indicates the position of the C-terminus of the predicted anchor sequence of Upd3 from *Dmel*. Black arrowhead indicates the position of the C-terminus of the predicted signal sequence of Upd3 from *Dyak*. (D) Phylogenetic tree showing the conservation of *upd3* between the different *Drosophila* species *D. melanogaster* (*Dmel*), *D. sechellia* (*Dsec*), *D. erecta* (*Dere*), *D. yakuba* (*Dyak*), *D. ananassae* (*Dana*), *D. pseudoobscura* (*Dpse*), *D. grimshawi* (*Dgri*), *D. virilis* (*Dvir*) and *D. mojavensis* (*Dmoj*) and their relationship to the *D. melanogaster* Upd and Upd2.

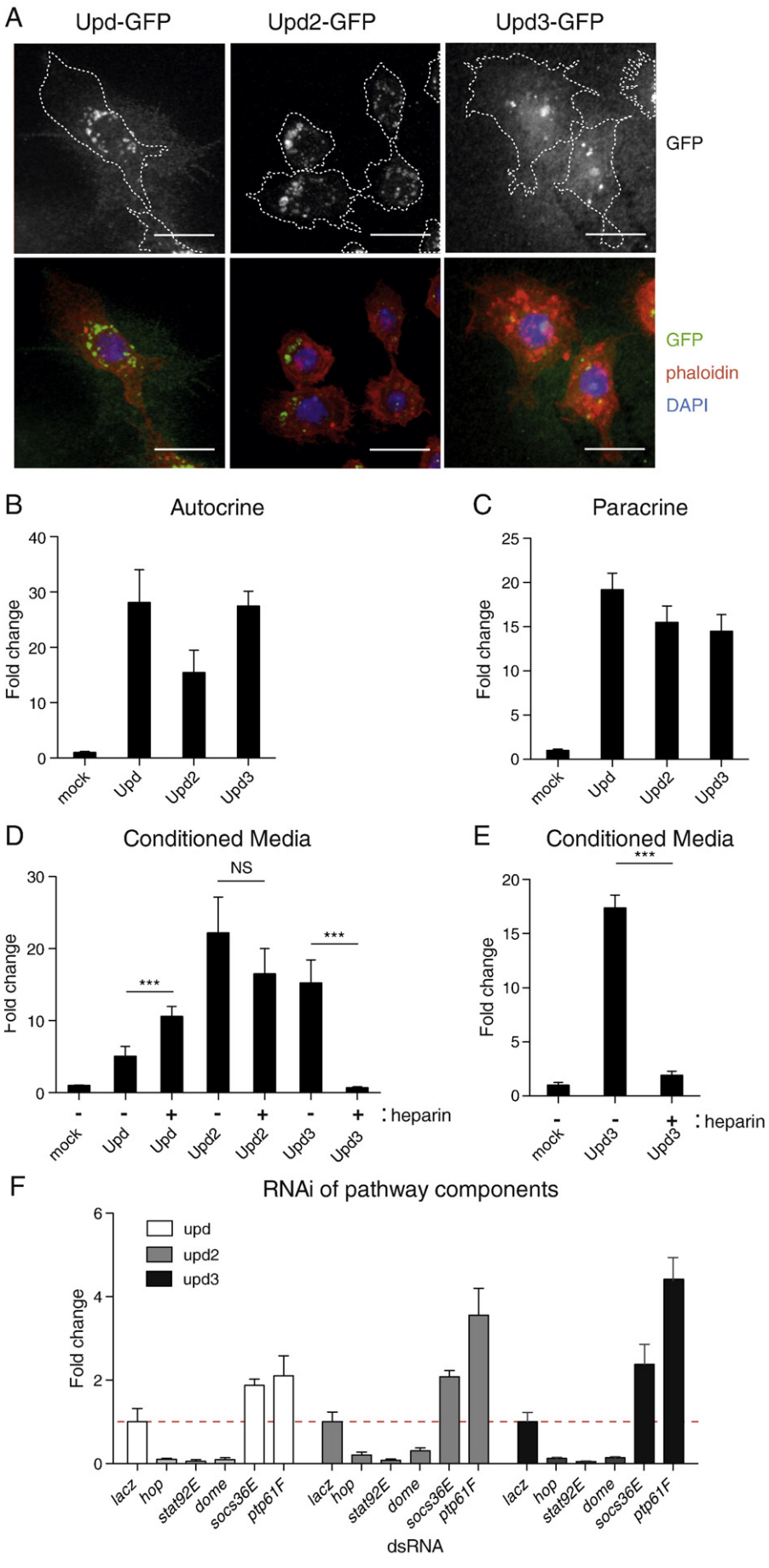
A
Upd-GFP
Upd2-GFP
Upd3-GFP
GFP
GFP
phaloidin
DAPI
B
Autocrine
Fold change
mock
Upd
Upd2
Upd3
C
Paracrine
Fold change
D
Conditioned Media
NS
***
***
: heparin
E
Conditioned Media
***
: heparin
F
RNAi of pathway components
upd
upd2
upd3
Fold change
lacz
hop
stat92E
dome
socs36E
ptp61F
dsRNA

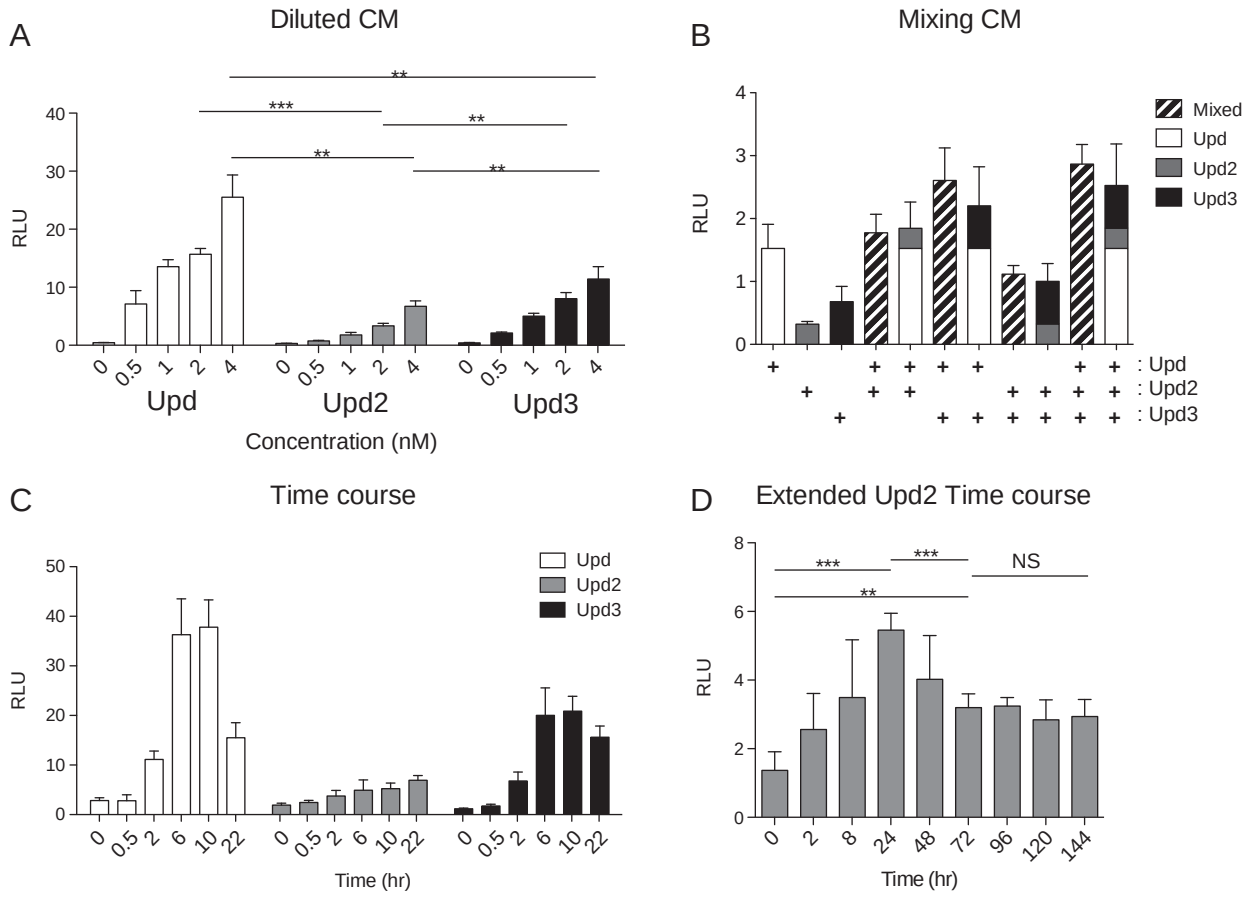

Fig. 3. JAK/STAT reporter activity in response to measured concentrations of ligand. (A) *6x2xDrafLuc* JAK/STAT reporter activity in response 24 h stimulation by the indicated ligand concentrations (0–4 nM). (B) *6x2xDrafLuc* JAK/STAT reporter activity in response to 24 h stimulation by 1 nM of the ligands indicated. The pathway activation is shown in response to mixing conditioned media for the ligands indicated (diagonal bars) or the total activation in response to 1 nM of each of the ligands individually. (C–D) *10xSTATLuc* reporter activity measured is in response to a 30 min pulse of 4 nM of the ligand indicated followed by incubation in normal (unconditioned) media for the times shown. (C) Response to 4 nM of Upd, Upd2 and Upd3 between 0 and 22 h of incubation. (D) Response to 4 nM Upd2 between 0 and 144 h of incubation. ** p = 0.01 to 0.001, *** p < 0.001, NS = not significant. Activity expressed as RLU—relative light units.

Tissue culture-based assays have shown that Upd3 interacts with the ECM, but at the same time is capable of conditioning media. In vertebrates, many cytokines and chemokines, including known activators of JAK/STAT signalling such as IFN-γ and GM-CSF bind to glycosaminoglycans (GAGs) via a heparin-binding domain [31]. It is thought that this interaction may assist in the immune response by recruiting immune cells to the area where the cytokine is bound [32]. It is interesting that Upd and Upd3 both adhere to the ECM yet respond differently to the addition of heparin, with Upd being released and solubilised while Upd3 activity is almost completely ablated. While low levels of conservation make it difficult to relate this result to JAK/STAT pathway ligands present in higher organisms it is interesting to note that IFN-γ is inhibited by heparin in humans whereas other heparin-binding cytokines such as IL-6 and IL-2 are not [23] suggesting that differences in heparin sensitivity may be physiologically important and evolutionarily conserved.

This is the first report that has described the quantification of the Upd-like ligands and this advance has allowed us to determine the ability of each ligand to activate the JAK/STAT pathway. Although care must be taken extrapolating results obtained from tissue culture systems, Upd2 was consistently found at significantly higher levels in conditioned media compared to Upd and Upd3. Although there could be differences in transfection efficiency, this finding supports the theory that many Upd and Upd3 are associated with the ECM while Upd2 is freely secreted into the media. Addition of 0.5–4 nM of each ligand to cells containing a JAK/STAT pathway reporter also showed that Upd has the highest specific activity being able to stimulate the *6x2xDrafLuc* reporter (and by inference JAK/STAT signalling) to higher levels than Upd3 and Upd2. However, a time-course experiment also revealed that the temporal response to Upd2, while lower, lasted significantly longer than for Upd or Upd3. It is possible that differences in ligand/receptor interaction or possibly trafficking of Upd2-activated receptor complexes through the endocytic machinery [33] may explain the differing response to these ligands. Alternatively, it is also possible that the lower level of stimulation elicited by Upd2 may be insufficient to trigger negative feedback pathways normally

Fig. 2. Secretion and signalling of the Upd-like ligands. (A) Kc_{167} cells transfected with the indicated GFP fusion proteins. Localisation of ligand–GFP is seen as white in upper panels and green in lower panels. Cells stained with Hoechst (blue) to mark nuclei and phalloidin (red) to outline the morphology of the cell. Cellular outlines are marked in upper panels by the dotted white lines. (B–E) Luciferase reporter assays. JAK/STAT activity is reported by *6x2xDrafLuc*. Fold change in response to autocrine (B), paracrine (C) and conditioned media produced with or without heparin (D) as well as media conditioned with Upd3 with heparin added (E). Y-axis is expressed as the fold change compared to mock treated samples. Significances are calculated using *t*-test with **p = 0.01 to 0.001, ***p < 0.001, NS p > 0.05. All samples in B and C represent p < 0.001 compared to mock control. (F) JAK/STAT pathway reporter activity following RNAi-mediated knockdown of canonical pathway components. Autocrine stimulation by each ligand, Upd, Upd2 or Upd3 is shown by white, grey and black bars respectively. Activity is expressed as the fold change compared to the response following *lacZ* knockdown (marked by red dashed line). All dsRNAs resulted in p < 0.001 when statistically analysed by *t*-test comparing to *lacZ* treatment for that ligand.

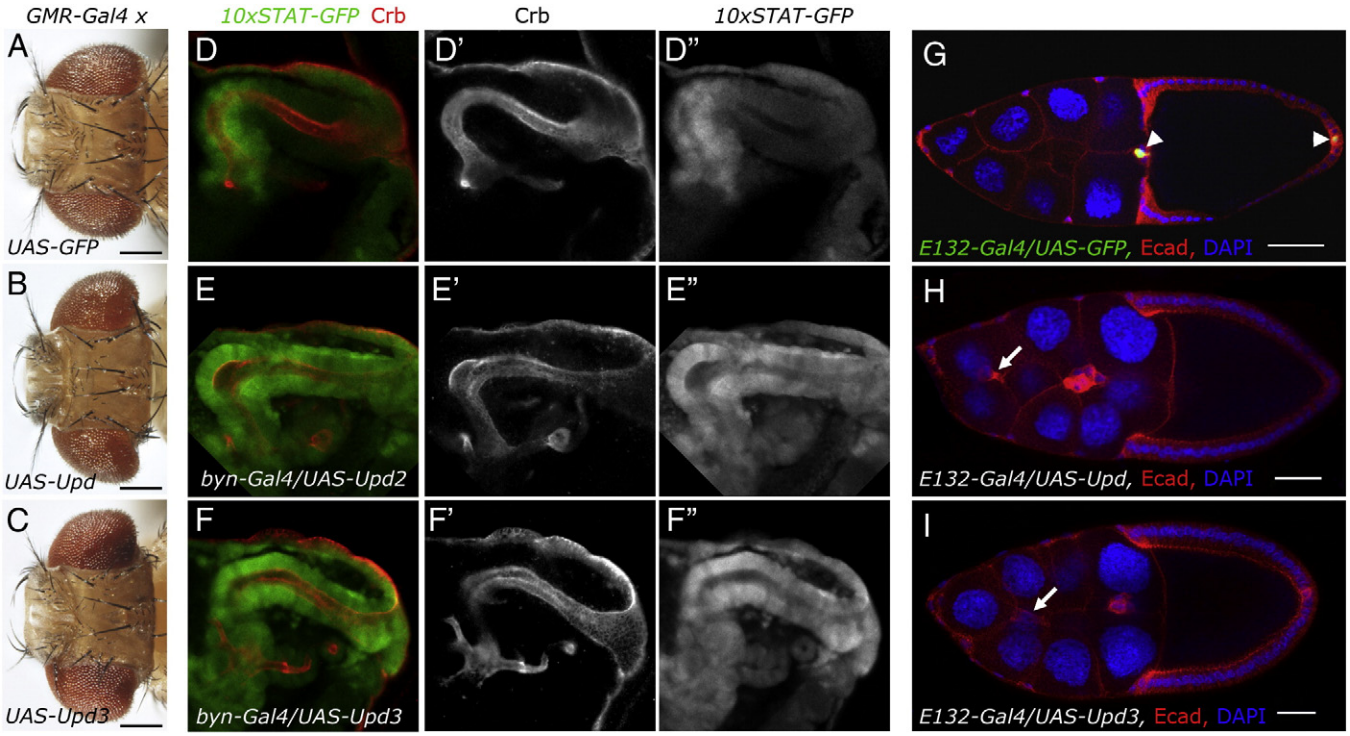

Fig. 4. Effects of ectopic Upd3 expression *in vivo*. (A–C) Results of *GMR–Gal4* driven *UAS–GFP*, *UAS–Upd* and *UAS–Upd3* on eye size. (D–F) *10xSTAT–GFP* activation (green) in the embryonic hindgut in response to *byn-Gal4* driven *UAS–Redstinger* (not shown—see Supplemental Fig. 1B), *UAS–Upd* and *UAS–Upd3*. Hindgut morphology marked by anti-Crb (red). (G–I) Effect of *E132–Gal4* driven *UAS–GFP* (green in G, arrow heads), *UAS–Upd* and *UAS–Upd3* on ovary border cell migration. Cells stained with Hoechst (blue) to mark nuclei and anti-DE-Cad (red). White arrows mark the presence of delayed supernumerary border cells.

responsible for shutting down pathway signalling. Ultimately further research will be required to establish the basis of this extended stimulation.

In addition to our studies into the mechanisms of Upd3 signalling *ex vivo*, we have also identified a P-element, *P[XP]d004951*, as a *UAS–Upd3* and used this to demonstrate the ability of Upd3 to activate JAK/STAT signalling *in vivo*. Ectopic expression in the eye-disc using *GMR–Gal4* results in an increase in eye size, similar to that observed following Upd mis-expression [5]. Thus suggesting that signalling via Upd3 is sufficient to drive cellular proliferation. Furthermore, driving Upd3 expression exclusively in the pole cells of the ovary using *E132–Gal4*, results in recruitment of excess cells to the border cell cluster. This phenotype is characteristic of Upd overexpression [28] and requires non-autonomous signalling of the ligand from the pole cells to the surrounding follicle cells. The ability of overexpressed Upd3 to phenocopy this effect confirms that Upd3 is capable of signalling non-autonomously *in vivo*.

4. Experimental procedures

4.1. Protein alignments

Genomic organisation, sequence alignments and searches of *upd*-like genes in other *Drosophila* species were undertaken using the tools available at http://flybase.org/. Alignments and phylogenetic trees were generated using DNA Star (DNASTAR Inc.) software. Signal sequence prediction used the SignalP [21] via a web interface available at http://www.cbs.dtu.dk/services/SignalP/ while identification of potential N-glycosylation sites was performed at http://www.cbs.dtu.dk/services/NetNGlyc/.

Table 1
Effect of ectopic gene expression on border cell migration.

Slbo–Gal4 x	% Normal	% Delayed
UAS–GFP ($n=143$)	97.9	2.1
UAS–Upd ($n=82$)	14.4	85.6
UAS–Upd3 ($n=142$)	50.5	49.5

Percentage of stage 10 ovaries scored with normal or delayed migrating border cells.

4.2. Cloning

The Upd3 expression construct was generated by amplifying the open reading frame of Berkeley *Drosophila* Genome Project clone, IP08763 (http://www.fruit fly.org/index.html) using the primers CAGGTACCAACATGACGACAGCTGACCGCCCG and GTTAGATCTAGTTT CTTCTGGATCGCCTTTG. PCR product was trimmed with Asp718 and BglII and ligated into *pBS–EGFP(B)* cut with Asp718 and BamHI. *upd3–GFP* was then excised inserted into a *pAc* backbone using Asp718 and XbaI sites to produce *pAc–Upd3–GFP*.

4.3. Luciferase assays

Drosophila Kc_{167} cells were maintained in Schneider's medium (Gibco), 10% heat inactivated FBS (Sigma) and 5% Pen-Strep (Gibco) at 25 °C. Autocrine luciferase assays were carried out as in Ref. [22] using *pAc–Upd–GFP*, *pAc–Upd2–GFP* or *pAc–Upd3–GFP*. Paracrine assays were carried out as described in Ref. [16] with signal-receiving cells transfected with *6x2xDrafLuc* reporter, *pAc–Renilla* and empty *pAc* and signal sending cells transfected with *pAc* (empty vector), *pAc–Upd–GFP*, *pAc–Upd2–GFP* or *pAc–Upd3–GFP* and incubated for 3 days before cell lysis and luciferase measurement. Conditioned media was produced as described in Ref. [16]. Briefly, signal-receiving cells transfected as for the paracrine assays were treated with 50 µl conditioned media (of the specified concentration) in 96 well plates. The cells were incubated for a further 1–3 days, lysed and measured for luciferase activity. For the time-course the *6x2xDrafLuc* reporter was substituted for 80 ng *10xSTATluc* and empty vector. Cells were treated with conditioned media containing 4 nM of each ligand for 30 min, washed with medium

supplemented with 10% FBS and incubated for the time indicated before cell lysis and luciferase activity measurement as described in Ref. [22].

4.4. Anti-GFP ELISA

100 µl of 1 µg/ml goat anti-GFP (Abnova) capturing antibody in 100 nM Sodium Bicarbonate was added to each well of a 96-well plate and incubated at 4 °C overnight. The plate was subsequently washed and blocked for 1 h with PBS + 0.5% Triton-X100 + 0.2% BSA. A recombinant GFP standard (Cell Biolabs) was added in triplicate at concentrations of 0. 0.125, 0.25, 0.5, 1, 2, 4 and 8 ng/ml to produce a standard curve. Each conditioned media sample was serial diluted (1:2) and 100 µl of each dilution was added to the plate in triplicate incubated at 4 °C overnight. The plate was washed with PBS + 0.2% BSA and incubated with 100 µl rabbit anti-GFP (kind gift of S.J. Foster, University of Sheffield) used at 1:2000 for 2 h at room temperature. This was then washed, incubated with 100 µl anti-Rabbit HRP (SignalChem) 1:5000 and incubated at room temperature for a further 1 h. 25 ml HRP buffer was mixed with 10 mg O-Phenylenediamine and 10 µl Hydrogen peroxide and 200 µl dispensed per well. This was incubated for a few minutes to develop colour before addition of 50 µl 2 M H_2SO_4 to terminate the reaction and measurement of absorbance at 492 nm.

4.5. Genetics

Drosophila were raised on standard cornmeal/agar food. For the qRT-PCR experiment, *P[XP]d04951* and *UAS–GFP* were crossed to *Actin–Gal4/CyO* and embryos collected on apple agar plates for 8–16 h. For ectopic expression in the *Drosophila* eye, *UAS–upd*, *P*[*XP*]*d04951* and *UAS–GFP* were crossed to *GMR–Gal4/CyO* at 25 °C. For expression in the ovary, *UAS–Upd*, *P*[*XP*]*d04951* and *UAS–GFP* were crossed to *E132–Gal4* or *Slbo–Gal4*. Embryos were incubated at 18 °C until flies hatched and incubated at 25 °C for a further 4 days before ovaries were dissected. For expression in the embryonic hindgut *UAS–Upd*, *P*[*XP*]*d04951* and *UAS–Redstinger* were crossed to *byn-Gal4/CyO* at 25 °C on apple agar plates and embryos collected after 13 h.

4.6. qRT-PCR

Embryos were dechorionated in 50% bleach and washed in ddH_2O. mRNA was extracted, cDNA prepared and RT-PCR carried out as described in Ref. [34], using the primers AACTGGATCGACTATCGCAAC and CTATGGCCGAGTCCTGGCTAC for *upd*, TACAAGTTCCTGCCGAACATG and ATGTGGCGGTACCAAGTCTTT for *upd2*, ACAAGTGGCGATTCTATAAGG and ATGTTGCGCATGTACGTGAAG for *upd3* and GACGCTTCAAGGGA CAGTATCTG and AAACGCGGTTCTGCATGAG for *rpl32*. PCR was performed in triplicate and normalised to *rpl32*.

4.7. Histology

For the visualisation of ligand, Kc_{167} cells were transfected with *pAc–Upd–GFP*, *pAc–Upd2–GFP* or *pAc–Upd3–GFP* fixed and stained as described in Ref. [16] using rabbit anti-GFP (Abcam) at 1:3000, Alexa-fluor anti-rabbit 488 conjugated secondary antibody (Molecular Probes) at 1:2000, Alexa Fluor 568 Phalloidin (Molecular Probes) at 1:100 and Hoechst at 1:10000 (Sigma). *Drosophila* ovaries were dissected and stained as described in Ref. [35] using anti-DCAD2 (DSHB) at 1:200, anti-rat Cy3 at 1:500 and Hoechst at 1:10000 (Sigma). Embryos were fixed and stained as previously described in Ref. [36] using anti-Crb (DSHB) at 1:10, Alexa Fluor anti-mouse 647 (Invitrogen) at 1:500 and FITC anti-GFP (Abcam) at 1:500. All fluorescent samples were visualised using a Zeiss LSM 510 confocal.

Supplementary materials related to this article can be found online at doi:10.1016/j.cellsig.2011.01.020.

Acknowledgements

We would like to thank Norbert Perrimon for the 10xSTATLuc reporter, the Bloomington Stock Centre for the *P*[*XP*]*d04951* stock and Prof. Simon J. Foster for the anti-GFP antibodies. Also, Susan Smith provided valuable comments on the manuscript while Richard Wells and Nina Bausek provided advice for *in vivo* experiments. Confocal imaging was undertaken in the Wellcome Trust supported Sheffield Light Microscopy Facility. MZ is a Cancer Research UK Senior Cancer Research Fellow and both VW and MZ are members of the MRC Centre for Developmental and Biomedical Genetics.

References

[1] W.X. Li, Trends Cell Biol. 18 (11) (2008) 545.
[2] R.L. Levine, G. Wernig, Hematol. Am. Soc. Hematol. Educ. Program 233–239 (2006) 510.
[3] V. Lacronique, A. Boureux, V.D. Valle, H. Poirel, C.T. Quang, M. Mauchauffe, C. Berthou, M. Lessard, R. Berger, J. Ghysdael, O.A. Bernard, Science 278 (5341) (1997) 1309.
[4] S.Y. Lai, E.E. Childs, S. Xi, F.M. Coppelli, W.E. Gooding, A. Wells, R.L. Ferris, J.R. Grandis, Oncogene 24 (27) (2005) 4442.
[5] E.A. Bach, S. Vincent, M.P. Zeidler, N. Perrimon, Genetics 165 (3) (2003) 1149.
[6] S.H. Jung, C.J. Evans, C. Uemura, U. Banerjee, Development 132 (11) (2005) 2521.
[7] R.P. Sorrentino, J.P. Melk, S. Govind, Genetics 166 (3) (2004) 1343.
[8] N.I. Arbouzova, M.P. Zeidler, Development 133 (14) (2006) 2605.
[9] L. Gregory, P.J. Came, S. Brown, Semin. Cell Dev. Biol. 19 (4) (2008) 407.
[10] H.W. Chen, X. Chen, S.W. Oh, M.J. Marinissen, J.S. Gutkind, S.X. Hou, Genes Dev. 16 (3) (2002) 388.
[11] S. Brown, N. Hu, J. Castelli-Gair Hombría, Curr. Biol. 11 (21) (2001) 1700.
[12] R. Binari, N. Perrimon, Genes Dev. 8 (3) (1994) 300.
[13] X.S. Hou, M.B. Melnick, N. Perrimon, Cell 84 (3) (1996) 411.
[14] R. Yan, S. Small, C. Desplan, C.R. Dearolf, J.E. Darnell Jr., Cell 84 (3) (1996) 421.
[15] D.A. Harrison, P.E. McCoon, R. Binari, M. Gilman, N. Perrimon, Genes Dev. 12 (20) (1998) 3252.
[16] J.C. Hombria, S. Brown, S. Hader, M.P. Zeidler, Dev. Biol. 288 (2) (2005) 420.
[17] H. Agaisse, U.M. Petersen, M. Boutros, B. Mathey-Prevot, N. Perrimon, Dev. Cell 5 (3) (2003) 441.
[18] J.L. Boulay, J.J. O'Shea, W.E. Paul, Immunity 19 (2) (2003) 159.
[19] P. Karsten, S. Häder, M.P. Zeidler, Mech. Dev. 117 (1–2) (2002) 343.
[20] Y.C. Tsai, Y.H. Sun, Genesis 39 (2) (2004) 141.
[21] O. Emanuelsson, S. Brunak, G. von Heijne, H. Nielsen, Nat. Protoc. 2 (4) (2007) 953.
[22] P. Müller, D. Kuttenkeuler, V. Gesellchen, M.P. Zeidler, M. Boutros, Nature 436 (2005) 871.
[23] W. Daubener, S. Nockemann, M. Gutsche, U. Hadding, Eur. J. Immunol. 25 (3) (1995) 688.
[24] G.H. Baeg, R. Zhou, N. Perrimon, Genes Dev. 19 (16) (2005) 1861.
[25] E.A. Bach, L.A. Ekas, A. Ayala-Camargo, M.S. Flaherty, H. Lee, N. Perrimon, G.H. Baeg, Gene Expr. Patterns 7 (3) (2007) 323.
[26] D.D. Iwaki, J.A. Lengyel, Mech. Dev. 114 (1–2) (2002) 71.
[27] C. Ghiglione, O. Devergne, E. Georgenthum, F. Carballes, C. Medioni, D. Cerezo, S. Noselli, Development 129 (23) (2002) 5437.
[28] D.L. Silver, E.R. Geisbrecht, D.J. Montell, Development 132 (15) (2005) 3483.
[29] G. Halder, P. Callaerts, W.J. Gehring, Science 267 (5205) (1995) 1788.
[30] P. Rorth, Mech. Dev. 78 (1–2) (1998) 113.
[31] R.E. Hileman, J.R. Fromm, J.M. Weiler, R.J. Linhardt, Bioessays 20 (2) (1998) 156.
[32] Y. Tanaka, D.H. Adams, S. Hubscher, H. Hirano, U. Siebenlist, S. Shaw, Nature 361 (6407) (1993) 79.
[33] O.M. Vidal, W. Stec, N. Bausek, E. Smythe, M.P. Zeidler, J. Cell Sci. 123 (Pt 20) (2010) 3457.
[34] S. Bina, V.M. Wright, K.H. Fisher, M. Milo, M.P. Zeidler, EMBO Rep. 11 (3) (2010) 201.
[35] D.L. Silver, D.J. Montell, Cell 107 (7) (2001) 831.
[36] N. Harden, M. Ricos, K. Yee, J. Sanny, C. Langmann, H. Yu, W. Chia, L. Lim, J. Cell Sci. 115 (Pt 10) (2002) 2119.